

Motion-Based Robotic Instrument Targeting Under C-Arm Fluoroscopy¹

Alexandru Patriciu^{1,2}, Dan Stoianovici, Ph.D.^{1,2}, Louis L. Whitcomb, Ph.D.²,
Thomas Jarrett, M.D.¹, Dumitru Mazilu, Ph.D.¹, Alexandru Stanimir, Ph.D.¹,
Iulian Iordachita, Ph.D.¹, James Anderson, Ph.D.⁴,
Russell Taylor, Ph.D.³, Louis R. Kavoussi, M.D.¹

Johns Hopkins University Baltimore, Maryland, USA

¹James Buchanan Brady Urological Institute, Johns Hopkins Medical Institutions
URobotics, JHBMC-D0300, 5200 Eastern Ave., Baltimore, MD 21224, USA dss@jhu.edu

²Department of Mechanical Engineering, Whiting School of Engineering

³Department of Computer Science, Whiting School of Engineering

⁴Department of Radiology, Johns Hopkins Medical Institutions

Abstract: We present a simple and precise robot targeting method under portable x-ray fluoroscopy based on image servoing. The method is implemented for needle alignment in percutaneous procedures using the PAKY-RCM robot developed in our laboratory. Initial clinical tests apply to the access of the renal collecting system.

Previously reported methods for computer assisted instrument targeting under fluoroscopy use complex robot-image registration algorithms. These approaches use static images of fiducial markers to estimate the robot-image coordinate mapping, which is then used for targeting. In contrast, we report a new method to directly perform targeting by using a marker located on the robot/end-effector and performing fluoro-servoing under continuous imaging. Three-dimensional targeting is achieved by performing the alignment in two dissimilar views acquired at arbitrary C-Arm orientations.

The percutaneous access implementation of this method provides automated alignment of the needle towards a surgeon specified target. Needle insertion is then controlled by the surgeon using side-view fluoroscopic feedback.

The proposed method offers increased accuracy, simplicity, and repeatability. Moreover, initial clinical experiments suggest that through the use of this method access time and radiation dose have been reduced as compared to normal manual procedures.

1 Introduction

Minimally invasive and noninvasive procedures are gaining increased popularity mainly due to reduced trauma and improved recovery time. One of the main problems encountered in minimally invasive procedures is, in contrast to open procedures, a dramatic reduction in the surgeon's visual ability. Radiological, ultrasonic, and magnetic resonance imaging techniques are employed to map anatomical geometry in intraoperative procedures [5,8,12].

Portable ultrasonic and fluoroscopy units (commonly termed C-Arms) are ubiquitous in modern operating rooms. Both of these affordable imagers provide real time two-

¹ Medical Image Computing and Computer-Assisted Intervention, October 11-14, 2000, Pittsburgh, PA, Lecture Notes in Computer Science, Springer-Verlag, Vol. 1935, pp. 988-998

dimensional (2-D) visualization. A common impediment in using these 2-D imagers is the lack of volumetric representation necessitating extensive surgical training for correct 3-D interpretation. The problem of “retrofitting” computer image-based 3-D navigation systems on commonplace C-arms is complicated by the fact that the vast majority of portable fluoroscopy systems do not provide encoding of the C-Arm position or orientation. This creates difficulty in estimating the pose of the imager with respect to the patient, thus complicating computer assisted procedures using this image information. Many solutions have been proposed for helping surgeons in performing fluoroscopy guidance [7,8]. For example, Navab et al. proposed an efficient algorithm [16,17] allowing for the complete reconstruction of volumetric anatomy using multiple 2-D images. Simultaneously, other researchers concentrated on the development of image guidance and registration techniques for various fluoroscopy guided interventions [7,8,18,19,20].

Most image guided procedures, such as percutaneous needle access, radio, and ultrasonic ablation require targeting of a specific instrument / probe at an exact organ location. The clinical outcome of these procedures significantly relies on targeting accuracy.

To address this problem, authors and others have reported computer-assisted instrument targeting based on the development of specialized image registration algorithms. Such methods commonly use at least two images of a spatial radio-opaque marker of complex geometry or a series of one-dimensional marks distributed on a defined pattern [4]. The x-ray projection of the markers is used to estimate the instrument-image coordinate mapping, which is then used for targeting. These algorithms compute the exact position of the target with respect to the instrument and the geometrical parameters of the imager [13], such as the source position, magnification factor, etc. In these procedures distortion correction and image calibration techniques may also be required for increased accuracy [4,13].

In contrast to these “fully calibrated” approaches, our approach is “uncalibrated” in the sense that the method achieves accurate needle placement without precise camera/imager calibration. For a discussion of the advantages and disadvantages of “uncalibrated” vision methods the reader is directed to [9].

Our “uncalibrated” approach is principally motivated by the technique we have frequently observed in use by experienced surgeons in performing manual needle access under fluoroscopy. Based on this observation, we have previously developed a targeting method for percutaneous needle access based on the needle superimposition over the target, calyx of the kidney [20]. This method was implemented using our PAKY needle driver and then updated with the addition of the RCM robot [22] and GREY supporting arm [14]. The system is used clinically in our institution and has proved to offer a substantial improvement over the manual approach [6]. In this method, however, targeting is performed by the surgeon controlling the robot.

This paper reports the development of a computer-controlled image-guidance technique for automated targeting using this system. The method uses fluoro-servoing (robot control based on direct image feedback from the C-Arm) in two arbitrary image views acquired at dissimilar C-Arm orientations. Similar guidance techniques have been successfully used for industrial robot guidance based on video camera images [1,3,11, 10,15].

We present the fundamentals of this new fluoro-servoing method, its application to needle guidance using the PAKY-RCM robot, and clinical application of this system for percutaneous renal access.

2. Methods

The system comprised of a surgical robot, a PC for image processing and robot control, and a C-Arm imager, is schematically represented in Figure 1. The digital C-Arm (OEC-9600) provides x-ray images under PC command. The image is acquired using a video card (Matrox Meteor). The robot is controlled from the same PC using a real-time motion control card (PCX-DSP8, by Motion Engineering, Inc.). The fluoro-servoing algorithm controls needle orientation based on radiological feedback.

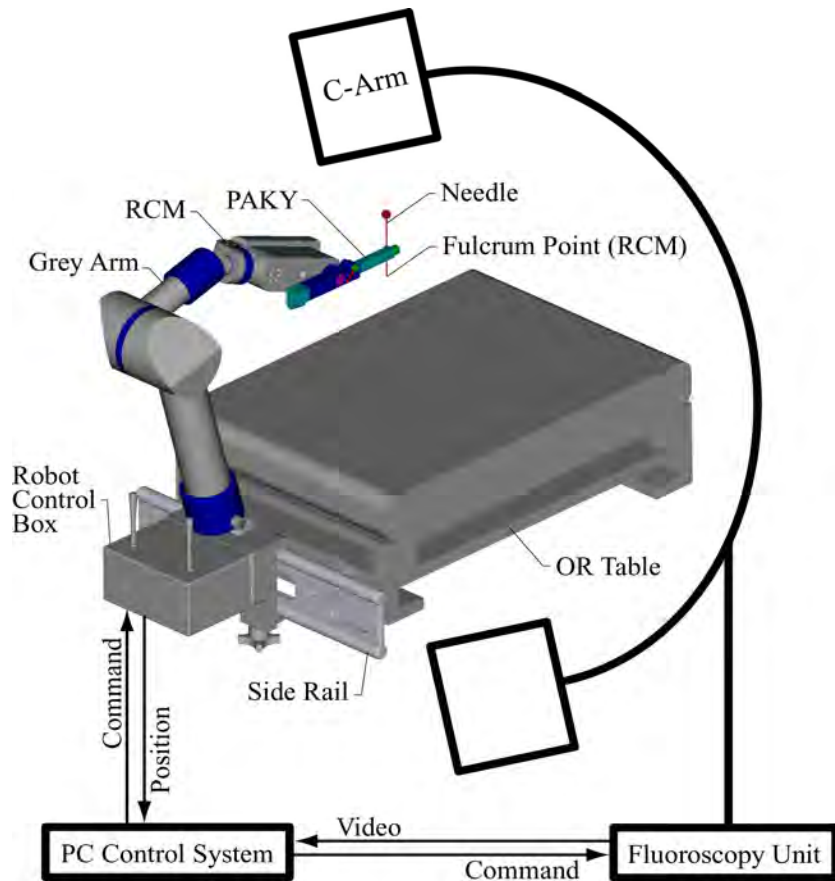


Figure 1: Schematic of system architecture

2.1 The Robotic System

The main component of the system is the PAKY-RCM robot comprising the needle driver PAKY [20] and the RCM robot [22]. PAKY (Percutaneous Access of the Kidney) is a radiolucent needle driver used to guide and actively drive a trocar needle in

percutaneous access procedures. Its radiolucent design allows for unobstructed visualization of the procedure needle and anatomical target. The original PAKY driver was constructed for the “Superimposed Needle Registration Method” [20]. For the present application, PAKY was redesigned to accommodate the proposed computer-guided servoing algorithm. This was realized by providing a thinner outline in the shape of a rectangular bar as illustrated in Figure 1.

The RCM (Remote Center of Motion) is a compact robot for surgical applications that implements a fulcrum point located distal to the mechanism [20,22]. The robot can precisely orient an end-effector (i.e. surgical instrument) in space while maintaining the location of one of its points. This kinematic architecture makes it proper for applications requiring a singular entry point such as laparoscopy and percutaneous access.

The robot assembly is supported into the Grey Arm [14] mounted to the operating table. This allows for positioning and steady support of the robot in close proximity of the operated organ. The PAKY-RCM assembly is capable of orienting a needle while maintaining its tip location. This gives the ability of aiming the needle at any desired target while priority setting the skin insertion point and positioning the needle tip at that location. Only two motions are thus required for orientating the needle about the fulcrum point. The proposed targeting algorithm takes advantage of this kinematic simplicity, as presented in the following section.

2.2 Fluoro-Servoing Instrument Orientation

Fluoro servoing is a particularization of visual servoing using x-ray fluoroscopy feedback. Visual servoing is a generic name for the class of robot control algorithms using image feedback for performing positioning and tracking operations [1,3,11,10,15].

The main difficulty in performing portable fluoroscopy computer-assisted procedures is the lack of information regarding the pose of the imager with respect to the patient. As a mobile unit, the C-Arm is moved and reoriented during the procedure to satisfy surgical needs. We propose a simple and accurate algorithm for instrument (needle) targeting independent of C-Arm orientation. The algorithm uses fluoro-servoing to orient the needle about a fulcrum point located at its tip.

Aiming the needle at a desired target requires needle alignment in two dissimilar views obtained from different C-Arm orientations. That is, orienting the needle so that it extends into the target in both views. Since alignments are performed sequentially, the second alignment should not deteriorate the first.

Each alignment is performed automatically by the guidance algorithm, which corrects the needle position based on image feedback. For facilitating the automatic detection of the needle into the image the needle has been equipped with a radio-opaque spherical ball at the free end, thus providing a well-discriminated signature. A pattern-matching algorithm running on the video acquisition board is used to rapidly locate the ball marker in the x-ray image. All calculations are performed in a fixed reference frame centered at the needle tip and oriented according to the initial position of the robot.

The principle of operation is schematically represented in Figure 2, illustrating the needle supported by the PAKY driver and positioned with the tip at the skin entry point (F). The central illustration is a 3-D representation whereas the two side views are x-ray projections of this space from View 1 and View 2 respectively, as indicated by the arrows. The figure presents the needle at different positions, which will be scanned during the two-phase alignment. In this motion the tip of the needle remains at the

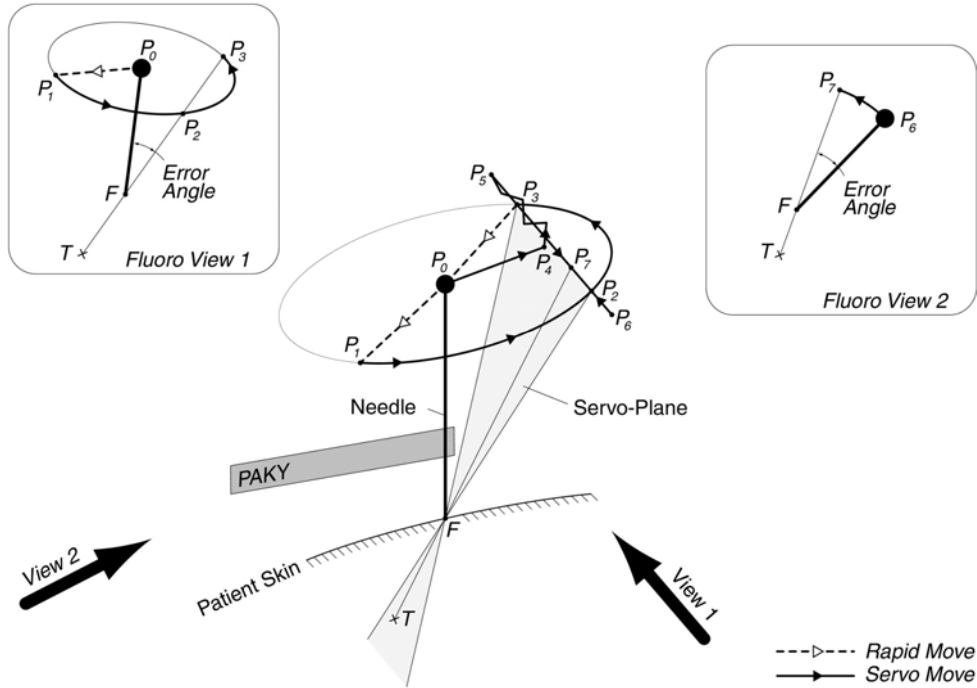


Figure 2: Fluoro-servoing instrument targeting

fulcrum point (F), while the needle end (the ball end) changes location from $P_0 \mapsto P_7$ as later described. The needle is initially located at P_0 . Targeting is achieved in two steps according to the C-Arm orientations View 1 and View 2.

View 1: A conical needle trajectory is used to obtain an initial estimate of the relative robot-image orientation. A rapid approach move of arbitrary direction P_0P_1 places the needle on the cone. The cone angle is set so that the target is located within the space swept by the needle extension. Starting from P_1 the needle is moved on the cone using incremental steps proportional to the orientation error. The error is given by the angle $180^\circ - \angle TFP_1$ measured in the x-ray projection (Figure 2). This proportional algorithm converges to the needle position P_2 , in which the needle at P_2F points towards the target T . Continuing on the conical path a second alignment is achieved at point P_3 in a similar manner.

The plane FP_2P_3 is the initial servo-plane. This plane has the property that at any position within the plane the needle maintains View 1 target alignment. Laboratory experiments showed that the identification accuracy of this plane was not consistent, errors depending on the distance of this plane from the start point P_0 . Explicitly, greater errors were encountered when points P_2 and P_3 were closely located at a side of the cone.

To overcome this problem, while maintaining a minimal cone angle, a correction of the servo-plane was implemented, following the $P_3 \rightarrow P_0 \rightarrow P_4 \rightarrow P_5 \rightarrow P_6$ path, as follows. The needle is rapidly brought to the start position P_0 and then moved in a plane FP_0P_4 perpendicular to the servo-plane. On this path fluoro servoing is employed to achieve accurate needle alignment at point P_4 . The algorithm uses the same angle-feedback

proportional control. The axis FP_4 is then used as a pivot about which the servo-plane is rotated for iterative corrections. From P_4 the needle is moved in the direction of the instantaneous servo-plane towards the point P_5 and then P_6 with a prescribed angular step. Target alignment is reevaluated at each step by searching transversally, and the orientation of the servo-plane is corrected accordingly. This is achieved by adjusting the servo-plane angle through the pivot axis FP_4 with an amount proportional to the angular targeting error. This new servo plane FP_5P_6 , is similar to the initial cone determined plane FP_2P_3 , however, it insures that the end points P_5 and P_6 are sufficiently spaced apart to render a consistent determination of the servo-plane and also averages errors over the multiple scan points on the $P_4 \rightarrow P_5 \rightarrow P_6$ trajectory. In our algorithm the limit points P_5 and P_6 were placed at a needle angle equal to the initial cone angle measured in the servo plane.

The servo-plane insures that independent of the needle orientation within this plane the needle is properly aligned to the target in the first view. Three-dimensional targeting requires the additional determination of an axis within this plane passing the fulcrum F and the target T , as presented next.

View 2: A second view is selected by reorienting the C-Arm. The orientation of this plane is arbitrary with the restriction that in this view the servo plane does not project into a line. The best precision is achieved if the view is normal to the servo-plane.

Needle alignment is performed by servoing the needle orientation within the previously determined servo-plane based on the same angle-error feedback, as represented in the x-ray projection Figure 2, View 2. The algorithm converges to the needle position FP_7 . In this orientation the target is located on the needle axis.

By using the servo-plane, the second view alignment preserves the first. Three-dimensional targeting is thus obtained by combining both 2-D alignments.

3 Results

The robotic system was adapted for the proposed method. A special design of the needle driver was implemented and integrated. The system using the servo-targeting algorithm was tested for accuracy and reliability using specially derived experiments and then clinically validated for percutaneous renal access.

3.1 Pre-Clinical Validation

For minimizing the radiation exposure during software design and evaluation the algorithm was initially developed and tested using a video camera mounted in a positioning stand. A white background and a black needle were used for achieving proper contrast. A 2mm spherical ball represented the target. Repeated tests revealed a targeting accuracy not greater than 0.5mm.

A second set of experimental tests was then performed in the operating room (Figure 3) using a digital C-Arm fluoroscope (OEC-9600). The ball-finder pattern-matching algorithm proved to be stable and robust under this imaging modality. Imager distortion was evaluated by constructing a template of equally spaced steel balls mounted on a thin radiolucent plate. For the imager used the overall distortion was found to be under 0.75 mm in a region next to the image center, this including the error of the ball-finder algorithm. Using the magnification function of the fluoroscope allowed for maintaining the field of view in the reduced distortion zone around the image center. Using a 2mm ball target located 80mm below the needle tip (fulcrum / skin entry point) the image



Figure 3: Experimental tests

guidance algorithm was evaluated for targeting accuracy. The maximum error in aiming the ball over 25 experiments was under 1.5mm. During the experiments the overall system comprising the robotic system, the imager, and the guidance algorithm proved to be reliable and consistently precise. The safety of the system for surgical applications is inherited from the kinematic design of the robotic component [22]. The PAKY-RCM presents decoupled orientation and needle insertion capabilities allowing for independent activation of the two stages. This insures that the needle may not be inadvertently inserted during the orientation stage and accidental reorientation may not occur during needle insertion.

The results of experimental trials, the safety of the mechanism, and the previous clinical experience using the RCM for percutaneous renal access at the Johns Hopkins Medical Institutions [6] and in numerous telesurgery transatlantic procedures [2,21] enabled us to confidently proceed with the clinical trials.

3.2 Clinical Application: Percutaneous Renal Access

In the initial application the fluoro-servoing targeting method was implemented for percutaneous renal access. A first case was recently performed in our institution (Figure 4).

For renal access the operating room and the patient are prepared as for the standard procedure. The patient is placed under total anesthesia. The fluoroscopy table is equipped with a special rigid rail. The robot is mounted onto the rail on the side of the targeted kidney and covered with a sterile bag. The needle driver is sterilized prior to the

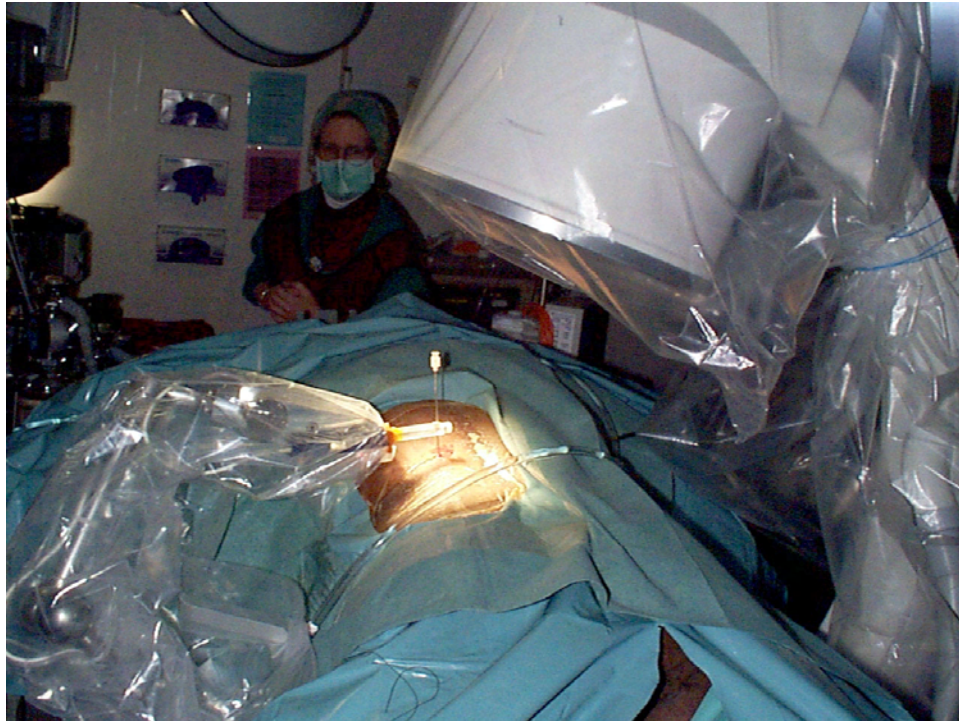


Figure 4: Fluoro-servoing percutaneous renal access at the Johns Hopkins Medical Institutions

operation. As for the manual procedure the C-Arm is positioned on the opposite side of the table and all steps prior to the needle access are performed as usual. First, the urologist chooses the skin insertion point as in the manual procedure and positions the robot assembly by manipulating the passive arm such that the needle tip (located at the fulcrum point of the RCM) is located at the chosen point. The C-Arm is oriented for proper kidney and needle visibility. Then the surgeon identifies the target calyx on the PC monitor by manually selecting a point on the image. The first view needle alignment is then automatically performed. The C-Arm is then rotated to a dissimilar view in which the surgeon identifies the target again. The second needle alignment is automatically performed. Using other C-Arm orientations the surgeon verifies needle targeting and performs needle insertion under direct lateral observation.

In all steps patient respiration is shortly stopped by the anesthesiologist during the image acquisition prior to target selection and during needle insertion. The patient may breathe in all other stages including servo targeting.

In the first operation performed the kidney was accessed on the first targeting attempt in less than 10 minutes. The needle, however, needed to be slightly retracted and reinserted again, as it initially pushed the kidney aside due to tissue deflection and needle bowing. This was not caused by targeting errors, since the small retraction and reinsertion properly aimed the target. This problem was also encountered due to the fact that for this patient the target was located on a peripheral lower pole calyx.

The total radiation exposure time of the patient during this procedure was 90 seconds. With future software development this could potentially be reduced by commanding the imager to strobe activate during the servo motion. This will be approached through collaborative work with the imager manufacturer. Even in the present implementation the total radiation was significantly reduced as compared to the common manual approach. This is due to the fact that the method offers a well-defined step-by-step algorithm eliminating the need for the problematic surgeon interpretation of volumetric anatomy.

4 Conclusions

In this paper we propose an algorithm for automatic instrument orientation under C-Arm guidance, and present preliminary experimental and clinical validation results. The method represents a simple solution to a common surgical problem. Manual fluoroscopy-guided interventions are normally based on trial and error requiring considerable surgical skill and operative training. Automatic targeting has the potential to reduce the required level of surgical experience and the variability among surgeons in performing this type of procedures. Given the increasing demand for image-guided interventions and the fact that the method employs the most common type of imager available in the operating room, the proposed approach could potentially yield widespread applications.

The success experienced in the first operation gives a preliminary method validation. Additional clinical cases are scheduled in the near future and will be presented in the literature. Implementation details and surgeon interface refinements will be performed accordingly. Different surgical procedures will also be explored in urology as well as other medical fields. The method may also prove useful for applications involving similar imaging equipment such as biplanar fluoroscopy units. As for the previous application of the RCM robot we will also investigate this method for telesurgery in a remotely operated setting.

References

1. Batista, J., Araujo, H., Almeida A.T.: "Iterative multistep explicit camera calibration", IEEE Transactions on Robotics and Automation. Vol 15, No 5., October 1999, p 897.
2. Bauer J.J., Stoianovici D., Lee B.R., Bishoff J., Caddeu J.A., Whitcomb L.L., Taylor R.H., Macali S., Kavoussi L.R., (1999), "Transcontinental Telesurgical Robotic Percutaneous Renal Access: Case Study", American Telemedicine Association (ATA) conference, Salt Lake City, Utah, abstract# 18D, April 18-21, 1999, Telemedicine Journal, 5(1):27, 1999.
3. Bernadero, A., Victor, J.S., "Binocular Tracking: Integrating perception and control", IEEE Transactions on Robotics and Automation. Vol 15, No 6., December 1999
4. Bzostek, A., Schreiner, S., Barnes, A.C., Cadeddu, J.A. Roberts, W., Anderson, J.H., Taylor, R.H., Kavoussi, L.R.: "An automated system for precise percutaneous access of the renal collecting system". Lecture Notes in Computer Science, Springer-Verlag, Vol. 1205, pp.299-308, 1997.
5. Brown R.A., Roberts T.S., Osborne A.G., "Stereotaxic Frame and Computer Software for CT-Directed Neosurgical Localization", Invest Radiol, 15:308-312, 1980.

6. Cadeddu, J.A., Stoianovici, D., Chen, R.N., Moore, R.G., Kavoussi, L.R., (1998), "Stereotactic mechanical percutaneous renal access", *Journal of Endourology*, Vol. 12, No. 2, April 1998, p. 121-126.
7. Desbat L., Champlébourg G., Fleute M., Komarek P., Mennessier C., Monteil B., Rodet T., Bessou P., Coulomb M., Ferretti G., "3D Interventional Imaging with 2D X-Ray Detectors", *Medical Image Computing and Computer-Assisted Intervention*, September 1999, Cambridge, England: Lecture Notes in Computer Science, Springer-Verlag, Vol. 1679, pp. 973-980, 1999.
8. Guéziec A., Kazanzides P., Williamson B., Taylor R.H., "Anatomy-Based Registration of CT-Scan and Intraoperative X-Ray Images for Guiding a Surgical Robot", *IEEE Transactions on Medical Imaging*, 17(5):715-728, 1998.
9. Hager, G., Hespanha, j., Dodds, Z., Morse, A.S., "What Tasks Can Be Performed with an Uncalibrated Stereo Vision System?", Submitted for review to IJCV.
10. Hager, G., Hutchinson, G., and Corke, P. A Tutorial Introduction to Visual Servo Control *IEEE Transactions on Robotics and Automation*, 12(5) pp. 651-670, 1996.
11. Hsu, L.; Aquino, P.L.S.: "Adaptive visual tracking with uncertain manipulator dynamics and uncalibrated camera", *Proceedings of the 38th IEEE Conference on Decision and Control* (1999), p. 5, vol (xvii+5325)
12. Ionescu G., Lavallée S., Demongeot J., "Automated Registration of Ultrasound with CT Images: Application to Computer Assisted Prostate Radiotherapy and Orthopedics", *Medical Image Computing and Computer-Assisted Intervention*, September 1999, Cambridge, England: Lecture Notes in Computer Science, Springer-Verlag, Vol. 1679, pp. 768-777, 1999
13. Jao J., Taylor, R.H., Goldberg, R.P., Kumar, R, Bzostek, A., Van Vorhis, R., Kazanzides, P., Gueznec, A., Funda, J., "A progressive Cut Refinement Scheme for Revision Total Hip Replacement Surgery Using C-arm Fluoroscopy", *Lecture Notes in Computer Science, MICCAI 1999*, pp. 1010-1019
14. Lerner, G., Stoianovici, D., Whitcomb, L., L., Kavoussi, L., R., (1999), "A Passive Positioning and Supporting Device for Surgical Robots and Instrumentation", *Medical Image Computing and Computer-Assisted Intervention*, September 1999, Cambridge, England: Lecture Notes in Computer Science, Springer-Verlag, Vol. 1679, pp. 1052-1061.
15. Molis, E., Chaumette, F., Boudet, S.: "2-1/2-D Visual Servoing", *IEEE Transactions on Robotics and Automation*. Vol 15, No 2., April 1999, p. 238
16. Navab, N., Bani-Hashemi, A., Nadar, M.S., Wiesent, K., Durlak, P., Brunner, T., Barth, K., Graumann, R.: "3D Reconstruction from Projection Matrices in a C-Arm Based 3D-Angiography system", 1998 MICCAI, *Lecture Notes in Computer Science, Springer-Verlag*, Vol. 1496, pp. 119-129, 1998.
17. Navab, N., Mitsche, M., Schutz, O.: "Camera-Augmented Mobile C-Arm (CAMC) Application: 3D Reconstruction Using a Low-Cost Mobile C-Arm", 1999 MICCAI, *Lecture Notes in Computer Science, Springer-Verlag*, Vol. 1679, pp. 688-705, 1999.
18. Potamiakos, P., Davies, B.L. Hilbert R.D. "Intra-operative imaging guidance for keyhole surgery methodology and calibration". *Proc. First Int. Symposium on Medical Robotics and Computer Assisted Surgery*, Pittsburgh, PA. P. 98-104
19. Potamiakos, P., Davies, B.L. and Hilbert R.D. "Intra-operative registration for percutaneous surgery", *Proc. Second Int. Symposium on Medical Robotics and Computer Assisted Surgery*, Baltimore, MD. Pp.156-164, 1995.

Motion-Based Robotic Instrument Targeting Under C-Arm Fluoroscopy

20. Stoianovici, D., Cadedu, J.A., Demaree, R.D., Basile H.A., Taylor, R. Whitcomb, L.L., Sharpe, W.N.Jr., Kavoussi, L.R.: "An efficient Needle Injection Technique and Radiological Guidance Method for Percutaneous Procedures", 1997 CVRMed-MrCas, Lecture Notes in Computer Science, Springer-Verlag, Vol. 1205, pp. 295-298, 1997.
21. Stoianovici, D., Lee, B.R., Bishoff, J.T., Micali, S., Whitcomb, L.L., Taylor, R.H., Kavoussi, L.R. (1998), "Robotic Telemanipulation for Percutaneous Renal Access", Journal of Endourology, Vol. 12, pp. S201.
22. Stoianovici, D., Witcomb, L.L., Anderson, J.H., Taylor, R.H., Kavoussi, L.R.: "A Modular Surgical Robotic System for Image Guided Percutaneous Procedures", 1998 MICCAI, Lecture Notes in Computer Science, Springer-Verlag, Vol. 1496, pp. 404-410, 1998.